JOURNAL OF GEOPHYSICAL RESEARCH, VOL. 88, NO. C7, PAGES 4381–4392, MAY 20, 1983

The Sampling Variability of Estimates of Spectra of Wind-Generated Gravity Waves

MARK DONELAN

National Water Research Institute, Canada Centre for Inland Waters, Burlington, Ontario, Canada L7R 4A6

WILLARD J. PIERSON

CUNY Institute of Marine and Atmospheric Sciences, City College of New York, New York, 10031

The sampling variability of spectra of wind-generated waves is tested against the predictions of the theory of waves as a stationary random quasi-Gaussian process. Both laboratory data, in which stationarity was prescribed, and field data, in which the external conditions were remarkably steady, were treated in the same way. It is demonstrated that the theory of stationary Gaussian processes provides accurate estimates of the sampling variability. For a record length of 17 min, commonly used in wave monitoring at sea, the uncertainties in the significant height and peak frequency estimates are approximately ±12% and ±5% respectively at the 90% confidence level. Furthermore, the height of the peak of the spectrum is generally overestimated.

1. INTRODUCTION

The study of waves in a wind-water tunnel has both advantages and disadvantages compared to the study of waves on the ocean. Disadvantages include the inability to model mesoscale and boundary layer aspects of atmospheric turbulence including lateral variations in the eddy structure of the winds. The wide range of the dimensions of the various wind-water tunnels that have been used can cause problems in scaling from one wind-water tunnel to another, much less from a wind-water tunnel to the free atmosphere over the ocean. Aspects of these difficulties can be found in the papers by *Resch and Selva* [1978], *Wu* [1979], *Pierson* [1980], *Wu* [1980], and *Mitsuyasu et al.* [1978] as examples.

A major advantage of a wind-water tunnel is the ability to keep conditions constant for a long enough time to obtain time series that provide relatively stable statistical estimates. It is possible to control and understand the effects of sampling variability in a wind-water tunnel, whereas in nature the winds and conditions of atmospheric stability vary as they will. The effects of actual variation of waves are mixed up with sampling variability effects in ways that are difficult to separate.

Techniques for the study of wave data by means of spectral analyses have been available since the work of *Tukey* [1949] as applied to waves by *Pierson and Marks* [1952]. The model of waves as a stationary random quasi-Gaussian process has been available for almost 30 years [*Neumann and Pierson*, 1966]. This method of analysis, as also given by *Blackman and Tukey* [1958], and its successor, the fast Fourier transform [*Cooley and Tukey*, 1965; *Cooley et al.*, 1967], predicts certain statistical and probabilistic properties of both the wave time histories and the spectra estimated from these time histories. To our knowledge, these probabilistic and statistical properties of wave time histories and the spectra estimated therefrom have not been fully verified. The theory has been more or less either accepted, or perhaps ignored, with the calculation of a spectrum treated as an end in itself and not as an aid for the understanding of the variability of the waves.

As an example, *Pierson* [1977] has raised objections to the current technique of scaling spectra according to f/f_m, where f_m is the frequency of the spectral peak. The frequencies of the spectral peaks are randomly varying quantities as are the spectral estimates and the significant wave heights computed therefrom.

The purposes of this paper are to verify the sampling variability effects that are present in spectral estimates computed from wave time histories and to suggest some of the difficulties that can result when spectra are scaled according to f/f_m in parameterizing these spectra.

To do this, we draw on two sets of wave data: one from a controlled laboratory experiment and the other from a fixed tower in Lake Ontario. Peak periods and significant heights from these two experiments differ by 1 and 2 orders of magnitude, respectively. Steady wind and fetch conditions were imposed on the laboratory experiment and gratefully accepted in the field observations. While we cannot claim laboratory steadiness in the natural wind, it will be seen that any unsteadiness in the wave field is buried in the sampling variability.

2. CONDITIONS OF THE EXPERIMENTS

The laboratory experiment was performed in the wind-wave tank at the Canada Centre for Inland Waters (CCIW), and the field observations were obtained from a tower in water of 12 m depth.

The wind-wave tank is 80 m long and 4.6 m wide. During the experiment, the water depth was 1.2 m and the air space above the still water level was 1.8 m high. The waves were measured at a fetch of 49.7 m. The wind at a height of 1.0 m above the still water level was 7.7 m/s. The friction velocity from previous measurements under the same conditions was 0.34 m/s, which corresponds to a wind at 10 m of 9.7 m/s. The wind speed and fetch were constant throughout the experiment, and the stability as indicated by the bulk Richardson number [*Donelan et al.*, 1974] was neutral.

The waves were recorded by means of a capacitance wire (1.1 mm diameter) and sampled every 0.1667 s by an A to D convertor with quantization steps of 0.07 mm. The Nyquist

Paper number 3C0175.
0148-0227/83/003C-0175$05.00

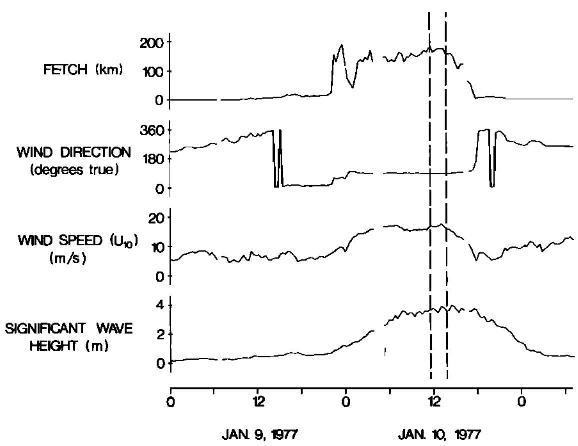

Fig. 1. Wind and wave-related parameters measured on the CCIW tower during the storm of January 10, 1977. The wave data analyzed in this paper were taken from the period enclosed by the vertical lines.

frequency was therefore 3 Hz. Sixteen sets of 1024 points were obtained for further analysis.

Although the laboratory waves were relatively small, Froude's law of scaling as used in model ship testing can be used to get an idea of the variability of the waves that might have occurred at sea. This could be accomplished by scaling time by a factor of 10 and height by a factor of 100. The frequencies of the wind-water tunnel spectra would be divided by 10 and the heights of the waves multiplied by 100. A 4 cm significant wave height in the wind-water tunnel would correspond to a 4 m significant height at sea. A frequency of 1 Hz (a period of 1 s) would correspond to a frequency of 0.1 Hz (a period of 10 s) at sea.

A record of natural wind-generated waves of this size was obtained from the CCIW tower 1.1 km offshore at the western end of Lake Ontario. Figure 1 is a record of the wind speed and direction, significant wave height, and average fetch during the storm of January 10, 1977. The fetch shown is the equally weighted average for each degree $\pm 15°$ on either side of the wind direction. The vertical lines enclose the section of data in which all four of these parameters were quite steady. The wave records to be discussed here were obtained from this 2½ h section. The eight time series selected in this study were chosen because the waves were high and because the data were expected to most nearly approximate the constant conditions in the wind-water tunnel. The variation of these four parameters is indicated by the highest and lowest values of their averages taken over 20-min sections:

15.7 ms	< wind speed	<	17.4 m/s
80°	< wind direction	<	86°
151 km	< fetch	<	182 km
3.35 m	< significant height	<	3.70 m

Wind speed and direction were measured at a height of 11.6 m above the still water level, and the atmospheric boundary layer was slightly unstable (the bulk Richardson number was approximately −0.01). The waves were recorded by means of a capacitance wire (4.8 mm diameter) and sampled every 0.2 s by an A to D convertor with quantization steps of 1.5 mm. In the following analysis, only every fourth sample is used. The Nyquist frequency was therefore 0.625 Hz. Eight sets of 1024 points each were obtained for further analysis.

Throughout the paper we present results from both field and laboratory data. In order to keep them in close juxtaposition, we retain the same figure and table numbers with the additional designation (field) or (laboratory) in the caption. In the text the numerical results from the controlled (laboratory) experiment are discussed directly with the equivalent field results in parentheses.

3. Brief Review of Theory

An ocean wave time history consisting of $N(= 2^n)$ points can be represented by the series of numbers in 1.

$$\eta(0),\ \eta(\Delta t),\ \eta(2\Delta t),\ \cdots\ \eta(p\Delta t),\ \cdots\ \eta((N-1)\Delta t) \qquad (1)$$

and, in turn, a fast Fourier transform would permit a representation as in (2)

$$\eta(p\Delta t) = \sum_{0}^{N/2} a_q \cos\frac{2\pi pq\Delta t}{N\Delta t} + b_q \sin\frac{2\pi pq\Delta t}{N\Delta t} \qquad (2)$$

The value of a_0 will typically be zero for a wave record without loss of generality, and $b_{N/2}$ will be zero. There will be a total of N values of the a and the b. The frequencies in the terms of (2) will range from 0 to $1/(2\Delta t)$, or from 0 to 3 (0.625) Hz. The Fourier coefficients are unique for each wave record, and (2) can be evaluated to reproduce (1) exactly.

The quantity

$$C_q^2 = \tfrac{1}{2}(a_q^2 + b_q^2) \qquad (3)$$

has a probability density function given approximately by

$$f(C_q^2)dC_q^2 = (\exp(-\ C_q^2/S_q))\ d(C_q^2/S_q) \qquad (4)$$

where

$$S_q = S\left(\frac{q}{N\Delta t}\right) = \int_{q/(N\Delta t)\ -\ 1/(2N\Delta t)}^{q/(N\Delta t)\ +\ 1/(2N\Delta t)} S(f)\ df \qquad (5)$$

for $1 \leq q \leq (N/2) - 1$, and with a slight modification of (5) for $q = 0$ and $q = N/2$, and where $S(f)$ is the 'true' but unknown spectrum of the random process which is assumed to be approximately a stationary Gaussian process. (Actually, there is a weight function involved in (5) such that the operation on the 'true' spectrum is not 'square.')

Equation (4) is a chi square distribution with two degrees of freedom with an unknown parameter, S_q. From (1) and (2), the estimate of the variance of the time history being analysed is given by (6)

$$\hat{\text{var}} = \frac{1}{N}\sum_{0}^{N-1} (\eta(p\Delta t))^2 = \sum_{1}^{N/2} C_q^2 \qquad (6)$$

which is an estimate of

$$\text{var} = \int_0^\infty S(f)\ df \qquad (7)$$

Given just one time history, say, a 1024 s (17 min, 4 s) sample, digitized once per second, the values of C_q^2 must be smoothed over frequency as, for example, in

$$\bar{C}_q^2 = \frac{1}{2R+1}\sum_{q-R}^{q+R} C_s^2 \qquad (8)$$

or more generally

$$\bar{C}_q^{\,2} = \sum_{q-R}^{q+R} \delta_s C_s^{\,2} \tag{9}$$

where

$$\sum_{q-R}^{q+R} \delta_s = 1 \tag{10}$$

so as to obtain a smoother function for the spectral estimates by means of the assumption, which may not always be correct, that the true spectrum is slowly varying. If the spectrum is slowly varying, then the values of $\bar{C}_q^{\,2}$ will be approximately distributed according to a chi square distribution with $2(2R + 1)$ degrees of freedom. Successive estimates will not be independent. Those elemental frequency bands that are $2R + 1$ bands apart will be independent.

With 16 (8) separate samples, the values of $C_{qk}^{\,2}$ ($k = 1$ to 16) could be averaged as in

$$\bar{C}_q^{\,2} = \frac{1}{16} \sum_{k=1}^{16} C_{qk}^{\,2} \tag{11}$$

to obtain an estimate of (5) with 32 degrees of freedom.

For a chi square distribution with 2 degrees of freedom, it can be shown that

$$P\left(0.103 < \frac{2C_q^{\,2}}{S_q} < 5.99\right) = 0.90 \tag{12}$$

and since the value of $C_q^{\,2}$ is known from the FFT, it follows that

$$P\left(0.334 < \frac{S_q}{C_q^{\,2}} < 19.42\right) = 0.90 \tag{13}$$

$$P(0.334\ C_q^{\,2} < S_q < 19.42\ C_q^{\,2}) = 0.90 \tag{14}$$

Given just one value of $C_q^{\,2}$, the value of the spectrum is not known to within a factor of 58 at the 90% confidence level. For the 16 pooled samples, the estimate of $\bar{C}_q^{\,2}$ has 32 degrees of freedom so that

$$P\left(20.1 < 32\frac{\bar{C}_p^{\,2}}{S_p} < 46.2\right) = 0.90 \tag{15}$$

thus

$$P\left(\frac{32}{46.2}\bar{C}_p^{\,2} < S_p < \frac{32}{20.1}\bar{C}_p^{\,2}\right) = 0.90 \tag{16}$$

or

$$P(0.69\ \bar{C}_p^{\,2} < S_p < 1.59\ \bar{C}_p^{\,2}) = 0.90 \tag{17}$$

The true spectrum is known now to within a factor of 2.3 at the 90% confidence level.

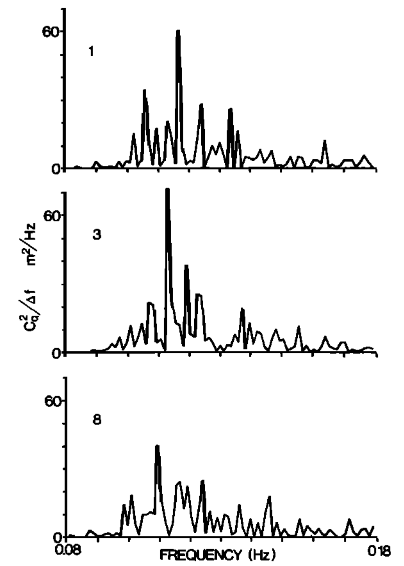

Fig. 2*b*. (Field) Three examples of the FFT spectra. Each spectral estimate has two degrees of freedom. The sample numbers are indicated on the figure.

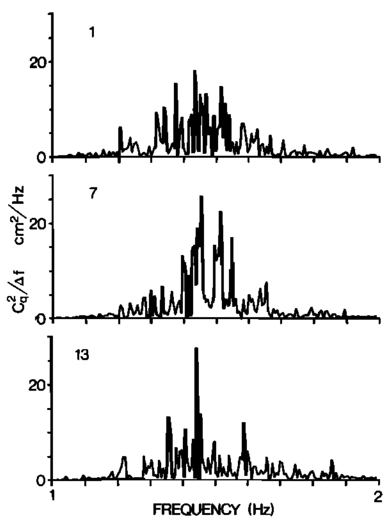

Fig. 2*a*. (Laboratory) Three examples of the FFT spectra. Each spectral estimate has two degrees of freedom. The sample numbers are indicated on the figure.

4. FFT's

Each of the 16 (8) sample records were analysed to obtain the FFT's. The values of $C_q^{\,2}\,(\Delta f)^{-1} = \hat{S}(f)$ were computed, tabulated, and graphed. Three of these graphs are shown in Figure 2 for samples 1 (1), 7 (3), and 13 (8), chosen to illustrate some of the extreme variability of FFT spectral estimates. Only the frequency range from 1 (0.08) to 2 (0.18) Hz is graphed. The spectrum above 2.0 (0.18) Hz had quite low values.

Table 1 gives the numerical values for the FFT spectra of the 16 (8) samples for the values somewhere in the general neighborhood of the peak of what might be the true but unknown spectrum. The individual values vary all the way from 0.02 cm² s (0.15 m² s) to 27.53 cm² s (71.59 m² s) for the 80 (40) numbers that are tabulated.

5. An Average Over the Sixteen (Eight) Samples

The 16 (8) sample FFT spectra can be averaged over values for each frequency in the FFT's. Those values for frequencies in the general vicinity of the peak of the 'true' spectrum are also given in Table 1. The 90% fiducial confidence intervals based on 32 (16) degrees of freedom from (17) are also given.

TABLE 1. FFT Spectral estimates in the vicinity of the peak

	q = 245, f = 1.436	q = 246, f = 1.441	q = 247, f = 1.447	q = 248, f = 1.453	q = 249, f = 1.459
			$\hat{S}(f)$		
			Laboratory		
Sample					
1	8.28	1.20	13.13	10.31	0.87
2	8.70	17.99	5.95	12.65	17.87
3	10.88	15.70	18.83	9.60	1.14
4	2.53	0.02	9.92	8.00	6.06
5	1.27	10.27	3.07	3.63	6.06
6	1.37	3.46	2.90	12.97	5.00
7	7.09	18.87	15.12	25.47	5.81
8	25.42	9.08	2.43	18.93	2.97
9	5.03	1.09	13.36	7.97	3.68
10	9.06	0.30	7.42	3.45	7.52
11	4.24	3.83	2.04	1.15	1.70
12	0.98	2.61	8.20	11.06	3.31
13	0.50	27.53	0.14	13.83	4.05
14	0.28	0.77	5.72	15.83	9.49
15	5.01	7.27	13.27	14.54	17.63
16	9.86	6.66	6.44	1.13	24.82
Average					
$C^2_q/\Delta f$	6.28	7.91	8.00	10.66	7.37
95%	10.01	12.61	12.76	17.00	11.75
5%	4.35	5.48	5.54	7.39	5.11
Nine-point filtered					
$\hat{S}_{ga}(f)$	7.19	7.28	7.59	7.33	7.02
95%	8.23	8.34	8.69	8.39	8.04
5%	6.28	6.36	6.63	6.40	6.13
	q = 89, f = 0.1088	q = 90, f = 0.1100	q = 91, f = 0.1112	q = 92, f = 0.1124	q = 93, f = 0.1136
			$\hat{S}(f)$		
			Field		
Sample					
1	17.36	0.94	3.49	20.64	13.40
2	3.72	38.73	31.53	3.72	23.07
3	4.19	5.71	0.85	71.59	23.24
4	27.35	11.50	21.06	30.44	1.79
5	0.15	23.40	4.40	39.34	24.09
6	13.20	45.71	32.25	0.54	9.84
7	19.62	56.36	47.46	22.00	4.41
8	40.06	15.55	6.62	0.73	5.65
Average					
$C^2_q/\Delta f$	15.71	19.15	18.46	23.63	13.19
95%	31.57	38.48	37.09	47.48	26.50
5%	9.55	11.65	11.23	14.37	8.02
Nine-point filtered					
$\hat{S}_{ga}(f)$	17.63	18.80	19.18	17.65	18.50
95%	21.62	23.05	23.52	21.64	22.68
5%	14.65	15.63	15.94	14.67	15.38

The highest and lowest three are underlined.

A graph of this spectrum is shown in Figure 3. There are now no exceptionally low spectral values between 1.2 (0.1) and 1.8 (0.14) Hz. The variability from point to point of the spectral estimates is still large. This result is not an ensemble average, nor has the need for the ergodic hypothesis been eliminated. The samples have simply been pooled under the assumption of stationarity.

6. SMOOTHING OVER FREQUENCY

Data from the ocean are rarely obtained for long enough time histories to be the equivalent of these 16 laboratory samples which each scale to 28 min, 27 s for the ocean, for a total sample of 7 h, 35 min. The alternative for a single sample is to smooth over frequency as in either of (8) and (9).

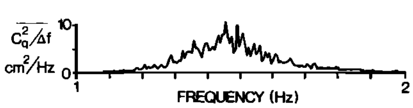

Fig. 3*a*. (Laboratory) The average for the 16 FFT spectra. Each spectral estimate has 32 degrees of freedom.

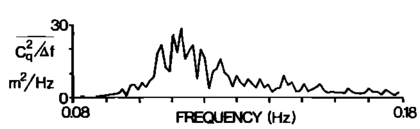

Fig. 3*b*. (Field) The average for the eight FFT spectra. Each spectral estimate has 16 degrees of freedom.

The original spectral analysis procedures of *Tukey* [1949] and *Blackman and Tukey* [1958] are effectively various versions of (9) for which the δ_s differ slightly. Also, only every Rth value of the spectrum, instead of that which can be obtained by means of a running average, is obtained.

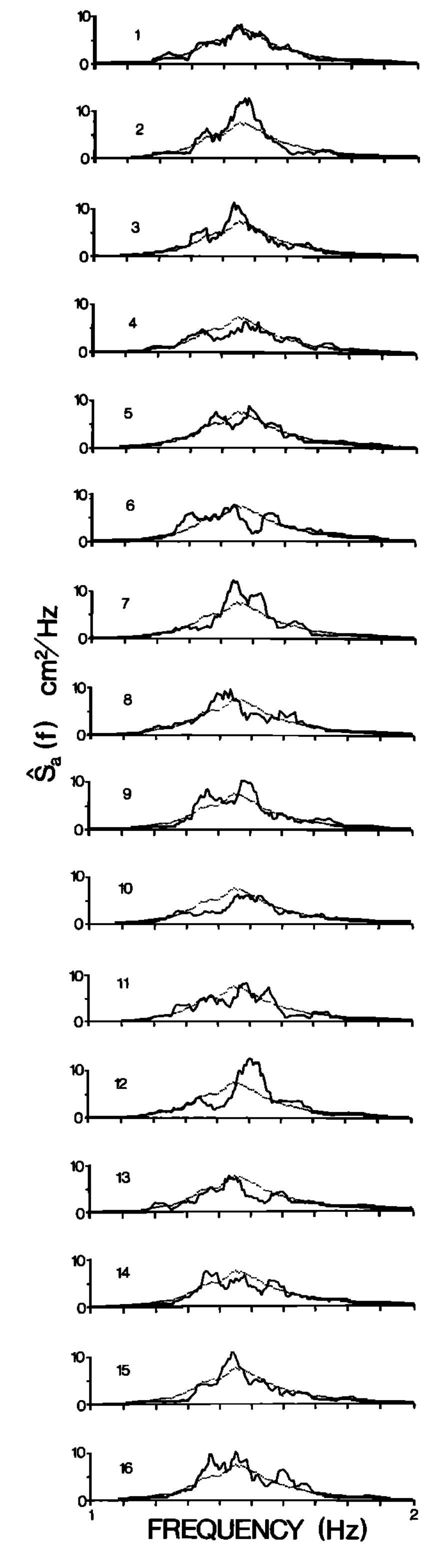

Fig. 4*a*. (Laboratory) FFT spectra averaged by a nine-point running average. Each spectral estimate has 18 degrees of freedom. The dotted line is the smoothed overall average from Figure 5. The sample numbers are indicated on the figure.

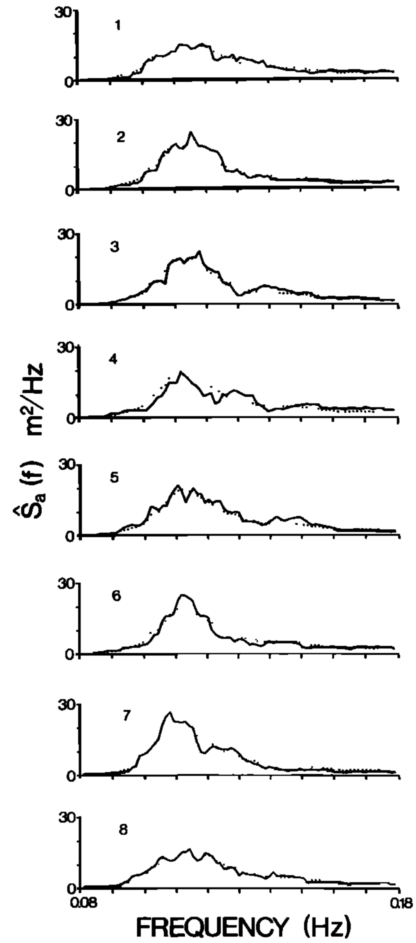

Fig. 4*b*. (Field) FFT spectra averaged by a nine-point running average. Each spectral estimate has 18 degrees of freedom. The dotted line is the smoothed overall average from Figure 5. The sample numbers are indicated on the figure.

Each of the 16 (8) sample records was averaged over frequency by means of a nine point running average so that if the spectrum is slowly varying over frequency, each spectral value has 18 degrees of freedom. The successive values are not independent so that the graphs of the spectra appear to have a certain pseudo-continuity. Every ninth point is independent.

These 16 (8) frequency smoothed spectra, $\hat{S}_a(f)$, are shown in Figure 4. (The circumflex is used throughout the paper to emphasize that the quantity is an estimate.) Only the frequency range from 1 (0.08) to 2 (0.18) Hz is graphed. These spectra still have multiple maxima. An analysis by means of the methods described in *Blackman and Tukey* [1958] for each of these samples might have yielded a value at every fourth dot (to be discussed shortly) with about 16 degrees of freedom such that every other value would be nearly independent. Connecting just every fourth value of the solid curves in these figures would yield spectra that would be deceptively smooth and that would often appear to have single maxima.

7. AN AVERAGE OF THE FREQUENCY SMOOTHED ESTIMATES

The next figure (Figure 5) can be obtained in either of two different ways. One is to use the running average of nine as

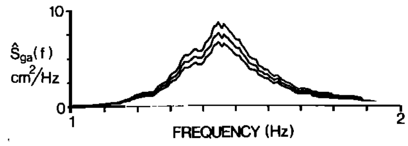

Fig. 5*a*. (Laboratory) The spectrum of Figure 3 smoothed by a nine-point running average. Each spectral estimate has 288 degrees of freedom and is within −12.7 to 14.5% of the 'true' spectrum at the 90% confidence level. The 90% confidence limits are also shown.

in (8) on the results of Figure 3. The other is to average frequency by frequency the 16 (8) results obtained by applying (8) to each sample; that is to average the spectra in Figure 4 so as to obtain a grand average, $\hat{S}_{ga}(f)$, based on a nine point running average over frequency and an average of all of the 16 (8) spectra. The result is still only an estimate of the 'true' spectrum, $S(f)$. Either way, the result is Figure 5, which is beginning to take on the properties that one might expect for the wave spectrum at this fetch and wind speed. A peak is located somewhere in the general vicinity of 1.45 (0.113) Hz.

Each spectral estimate has 18 × 16 (8) or 9 × 32 (16), or 288 (144) degrees of freedom (D). The 90% confidence interval for this large number of degrees of freedom is given [*Blackman and Tukey*, 1958, Table II] by

$$P(\alpha \hat{S}_{ga}(f) < S(f) < \beta \hat{S}_{ga}(f)) = 0.90 \tag{18}$$

where

$$\alpha \doteq 10^{-1/D^{1/2}} \tag{19}$$

and

$$\beta \doteq 10^{+1/D^{1/2}}$$

so that

$$P(0.873\ \hat{S}_{ga}(f) < S(f) < 1.145\ \hat{S}_{ga}(f)) = 0.90 \tag{20}$$

These α and β differ from Blackman and Tukey in that their $(D - 1)^{1/2}$ has been replaced by $D^{1/2}$, not significantly altering the level of approximation for $D > 10$. The spectrum is known to within about ±14.5 (21.1) % or a range of 27 (39) % at the 90% confidence level. These 90% confidence intervals are also given in Figure 5 and Table 1.

At both high and low frequencies a smooth curve between the two confidence intervals can be drawn. The exact location of the peak of the 'true' spectrum is an area of uncertainty even for 288 (144) degrees of freedom. The peak may lie somewhere between 1.42 (0.11) and 1.52 (0.12) Hz.

The dots on the spectra for the 16 (8) samples (Figure 4) are the values of this function at each of the frequencies for which it was computed (i.e., Figure 5 or $\hat{S}_{ga}(f)$). The spectra for the individual samples fluctuate above and below the spectra for $\hat{S}_{ga}(f)$. Sample spectrum number 12 (7) is dominantly above $\hat{S}_{ga}(f)$, and sample spectrum number 10 (4) is dominantly below. Instead of each of the 16 (8) sample spectra oscillating about the spectrum for the total sample at a fairly rapid rate, the sample spectra lie consistently above or below the spectrum of the total sample over substantial frequency intervals.

Table 1 also gives the values of $\hat{S}_{ga}(f)$ and the 90% confidence intervals for five spectral bands somewhere near the peak of the sample spectrum. For the 80 (40) illustrative values for the sample spectra, only 8 (4) fall within the confidence intervals for the appropriate frequency. The need for a large sample for the study of waves is demonstrated by the numbers in Table 1 and the graphs that have been shown.

8. Verification of the Chi Square Distribution

If S_q were known in (4), the random variable $x = C_q^2/S_q$ would be distributed according to $\exp(-x)$ for x greater than zero. The quantity, $\hat{S}_{ga}(f) = \hat{S}_{ga}(q/N\Delta t)$ can be used as an estimate of the true value and the hypothesis tested that the resulting values of x will have the exponential distribution.

This was done for values of q ranging from 196 (74) to 324 (170), or for frequencies from 1.148 (0.090) to 1.898 (0.208) Hz, for which $\hat{S}_{ga}(f)$ was greater than 7% of $\hat{S}_{ga}(f_m)$. The result was 2064 (776) values of x.

The histogram of these 2064 (776) values of x for a class interval 0.05 wide is shown in Figures 6*a* and 6*b* over the range from zero to four normalized to 1 at $x = 0$. Also shown is the theoretical curve, $\exp(-x)$. The sampling fluctuations about the theoretical curve are to be expected. Although not actually plotted the data continue past $x = 4$, and the last observation is in the range between 4.95 and 5.00. For this class interval the expected number is 0.44. The last four class intervals with data contain two observations so that, even for the highest values of x for this size sample, the distribution is fitted well.

This particular probability density function has the unique property that a variant of its cumulative density function is the same function as the probability density function as in (21)

$$F(x) = \int_x^\infty \exp(-\xi)\, d\xi = \exp(-x) \tag{21}$$

for $0 < x < \infty$.

A graph of $F(x)$ is shown in Figures 6*c* and 6*d*. The left-hand part of each horizontal line represents the ratio of the number of points having values of x in excess of that value to the total number of points in the sample. This ratio, except for sampling variability, should equal $\exp(-x)$ as shown by the dashed curve. The curve for the 2064 (776) sample values agrees very well with the theory.

The average value of all of the sample values of x was 0.9931 (0.9776) compared to an expected value of exactly one as in (22).

$$\int_0^\infty x \exp(-x)\, dx = 1 \tag{22}$$

The spectra of the 16 (8) samples satisfy the hypothesis that wind-generated waves are closely associated with the properties of stationary Gaussian processes.

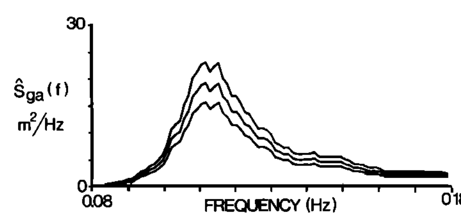

Fig. 5*b*. (Field) The spectrum of Figure 3 smoothed by a nine-point running average. Each spectral estimate has 144 degrees of freedom and is within −17.5 to 21.1% of the 'true' spectrum at the 90% confidence level. The 90% confidence limits are also shown.

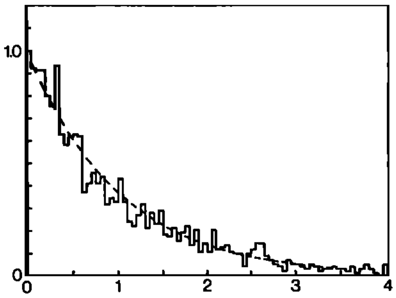

Fig. 6*a*. (Laboratory) Histogram of the ratio, x, of raw FFT spectral estimates (Figure 2) to the smoothed average spectral estimates (Figure 5). The class interval is 0.05, and the histogram has been normalized by its value in the first interval (0–0.05). The dashed line is exp $(-x)$.

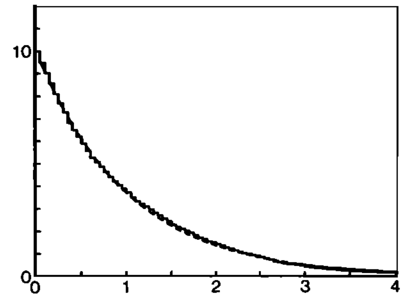

Fig. 6*c*. (Laboratory) A comparison of the inverse cumulative density for the normalized FFT random variables and the theoretical curve (dashed). The left inner corner of each step should be compared to the dashed curve for exp $(-x)$.

9. SAMPLING VARIABILITY OF THE SPECTRAL PEAK

The frequency of the spectral peak and the value of the spectral peak vary randomly from one of the 16 (8) subsamples to the other as shown in Figure 4. Table 2 gives the sample number, the frequency of the spectral peak as shown in Figure 4, the harmonic number, the value of the spectral estimate and its 90% confidence interval for that peak, and the value of the average of all spectra for that frequency as in Figure 5.

The confidence intervals on the spectral estimates for the peaks of the 16 (8) samples enclose the values of $\hat{S}_{ga}(f)$ for 11 (8) out of the 16 (8) samples. If $\hat{S}_{ga}(f)$ were, indeed, the 'true' spectrum, the chance that all 16 (8) would enclose the true value is 0.185 (0.430), that 15 would and one would not is 0.329 and that 13 would and three would not is 0.142, that 11 would and five would not is 0.014.

Picking the spectral peak for a spectral estimate from a sample with the degrees of freedom of one of the 16 (8) samples being studied in this paper and then scaling spectral properties according to f/f_m guarantees that the value of the spectral peak will be overestimated when many spectra fitted in this way are averaged. For the 16 (8) samples, all but 2 (2) are greater than the corresponding value for $\hat{S}_{ga}(f)$. There is almost a 50% chance that an estimate picked at random will be greater or less than the true value with 18 degrees of freedom. (For the chi square distribution the median is slightly less than the expected value.) There is only a 0.21 (14.4)% chance that values picked at random would be such that 14 (6) out of 16 (8) or more would be greater than the 'true' value. The bias in the procedure of scaling according to the spectral peak is shown by the disparity between the fact that 14/16 (6/8) of the values of the peaks of individual sample spectra lie above $\hat{S}_{ga}(f)$, whereas the chance at a particular frequency of being high so often is only 0.21 (14.4) %. Figure 7 illustrates the variability of the estimates of the spectral peak.

A given estimated spectrum $\hat{S}_1(f)$ will have a peak at some frequency, f_1. Other estimated spectra from the same stationary random process will have spectral estimates at f_1 that are not necessarily their peak values and that will more often than not be lower than $\hat{S}_1(f_1)$. If the peak spectral values $\hat{S}_a(f)$ in Table 2 are averaged and if the frequencies associated with these values are averaged, the result would be $\bar{S}(\bar{f}_m)$ as given in Table 2 and as indicated (asterisk) on Figure 7. This value is appreciably larger than and at a different frequency from $\hat{S}_{ga}(f_m)$ our best estimate of the 'true' spectral peak $S(f_m)$.

The ratio of $\hat{S}_a(f_m)$ to the value of $\hat{S}_{ga}(f)$ at the same frequency is also given in Table 2. The average of these ratios is 1.40 (1.21). Thus, picking the spectral peak and scaling to f/f_m biases the spectra toward values that are too high.

The frequency of the spectral peak varies from harmonic 231 (88), a frequency of 1.354 (0.1075) Hz to harmonic 256 (97), a frequency of 1.500 (0.1185). This is a variation of more than 10% in frequency. Even for the total sample, the true spectral peak could fall anywhere between harmonic 242 (90) and 259 (98) at the 90% confidence level (see Figure 5).

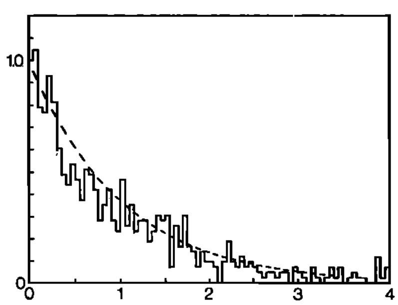

Fig. 6*b*. (Field) Histogram of the ratio, x, of raw FFT spectral estimates (Figure 2) to the smoothed average spectral estimates (Figure 5). The class interval is 0.05, and the histogram has been normalized by its value in the first interval (0–0.05). The dashed line is exp $(-x)$.

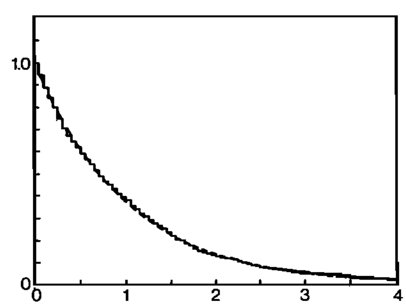

Fig. 6*d*. (Field) A comparison of the inverse cumulative density for the normalized FFT random variables and the theoretical curve (dashed). The left inner corner of each step should be compared to the dashed curve for exp $(-x)$.

TABLE 2. Sampling Variability of the Spectral Peak

	f (Hz)	q	Lower* (5% c.l.)	$\hat{S}_a(f)$*	Upper* (95% c.l.)	$\hat{S}_{ga}(f)$*	Y/N (R) H/L
				Laboratory			
Sample							
1	1.453	248	5.27	8.45	16.20	7.33	Y 1.15 H
2	1.477	252	7.99	12.81	24.56	7.03	N 1.82 H
3	1.430	244	7.16	11.48	22.01	6.92	N 1.66 H
4	1.471	251	4.10	6.57	12.59	7.16	Y 0.92 L
5	1.482	253	5.54	8.88	17.02	6.75	Y 1.32 H
6	1.441	246	4.75	7.62	14.61	7.28	Y 1.05 H
7	1.436	245	7.70	12.35	23.67	7.19	N 1.72 H
8	1.430	244	6.02	9.66	18.52	6.92	Y 1.40 H
9	1.471	251	6.36	10.20	19.55	7.16	Y 1.42 H
10	1.459	249	3.90	6.26	12.00	7.02	Y 0.89 L
11	1.488	254	5.17	8.29	15.83	6.60	Y 1.26 H
12	1.500	256	7.96	12.77	24.48	6.07	N 2.10 H
13	1.430	244	4.84	7.76	14.88	6.92	Y 1.12 H
14	1.354	231	4.69	7.52	14.42	4.60	N 1.63 H
15	1.436	245	6.84	10.97	21.03	7.19	Y 1.53 H
16	1.447	247	6.54	10.49	20.11	7.59	Y 1.38 H
Average							1.40
$\bar{f}_m$	1.450		$\bar{S}(\bar{f}_m)$	9.51			
$\hat{S}_{ga}(f_m)$	1.447	247	6.63	7.59	8.69	7.59	
				Field			
Sample							
1	0.1185	97	9.26	14.86	28.49	13.94	Y 1.07 H
2	0.1149	94	14.89	23.88	45.78	19.06	Y 1.25 H
3	0.1173	96	13.93	22.35	42.84	15.78	Y 1.42 H
4	0.1112	91	11.77	18.88	36.19	19.18	Y 0.98 L
5	0.1100	90	13.11	21.02	40.29	18.80	Y 1.12 H
6	0.1112	91	15.54	24.92	47.77	19.18	Y 1.30 H
7	0.1075	88	16.67	26.74	51.26	16.70	Y 1.60 H
8	0.1136	93	10.42	16.72	32.05	18.50	Y 0.90 L
Average							1.205
$\bar{f}_m$	0.1130		$\bar{S}(\bar{f}_m)$	21.17			
$\hat{S}_{ga}(f_m)$	0.1112	91	15.94	19.18	23.52	19.18	

* Laboratory in cm^2/Hz; field in m^2/Hz.

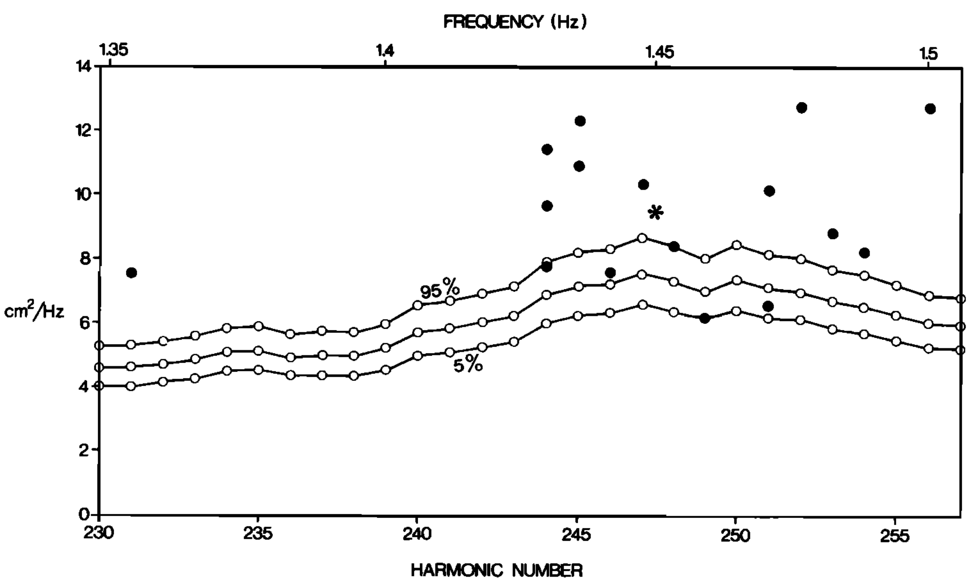

Fig. 7*a*. (Laboratory) The values of the smoothed average spectrum and its 90% confidence interval (Figure 5) with the peak values of the smoothed individual spectra (Figure 4). The average of the peaks of the 16 individual spectra $\bar{S}(\bar{f}_m)$ is indicated by an asterisk.

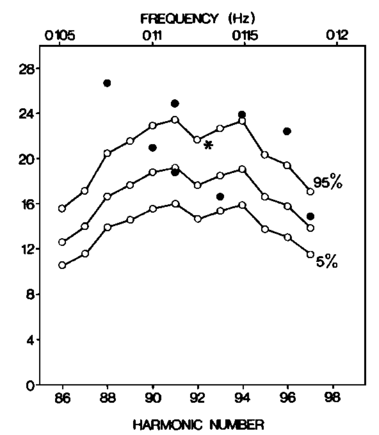

Fig. 7*b*. (Field) The values of the smoothed average spectrum and its 90% confidence interval (Figure 5) with the peak values of the smoothed individual spectra (Figure 4). The average of the peaks of the eight individual spectra $\bar{S}(\bar{f}_m)$ is indicated by an asterisk.

Thus, the predictions of *Pierson* [1977], that the spectral peak is an overestimate of the true spectral shape near the peak and that the frequency of the spectral peak varies randomly about a value estimated by combining the entire data sample, are verified.

Portions of a study by *Günther* [1981] also demonstrate exactly the same features. *Günther* [1981] assumed a JONSWAP [*Hasselmann et al.*, 1973, 1976] spectral form defined by the five JONSWAP parameters with the frequency of the spectral peak f_m normalized to a dimensionless form $f_m{}^* = f_m/\Delta f$, where Δf is the spectral resolution. For that spectral resolution, each spectral estimate was assumed to have 30 degrees of freedom. A set of spectra was generated by Monte Carlo techniques such that each band had a chi square distribution with an expected value defined by the chosen JONSWAP spectral shape.

This set of Monte Carloed spectra was then used to recover the five JONSWAP spectral parameters. For example, γ was computed from each of the simulated spectra, and the average value of γ was obtained. The values of $f_m{}^*$ were found and averaged to produce the average value of $f_m{}^*$, and so on. The parallelism to our present study is clear. *Günther* [1981] also derived the theoretical probability density functions for the distributions of the JONSWAP parameters and compared the statistics of the Monte Carlo simulations with the derived theory.

The theoretical analysis and the Monte Carlo simulations both demonstrated that recovered values of γ were always significantly larger than the input values of γ. The results are summarized in Table 3 for three spectral shapes, with spectrum III having the form of the fully developed sea given by *Pierson and Moskowitz* [1964]. Each of the three spectra simulated by Monte Carlo methods had the input parameters as listed. The random values of the frequency of the spectral peak averaged nearly to the input value of the frequency of the spectral peak. The average value of the values of the spectrum at the randomly varying frequencies of the spectral peaks did not yield the input value of γ. In fact, as Table 3 shows, the output values of γ were 9% and 22% too high for spectrum I, 28% and 40% too high for spectrum II, and 46% and 50% too high for spectrum III depending on whether the theory or the Monte Carlo results were used. Also σ_a and σ_b would result for the output spectrum for input spectrum III but, by definition, they do not exist for the input spectrum.

The three spectral shapes in Table 3 correspond to a sharply peaked spectrum (I), a fairly sharply peaked spectrum (II), and the broadly peaked spectrum of Pierson and Moskowitz (III). The variances and standard deviations of the JONSWAP parameters were also found. For the Monte Carlo simulations for spectra I, II, and III, $f_m{}^*$ equaled 16.9 $\pm$ 0.37, 48.9 $\pm$ 1.28, and 26.0 $\pm$ 1.83 for 2.2, 2.6, and 7.1% variability of the location of the spectral peak, respectively. Similarly, the values of γ were 4.02 $\pm$ 0.91, 4.61 $\pm$ 0.78, and 1.50 $\pm$ 0.54 for 23, 17, and 36% variability, respectively.

Had Günther averaged all of the spectra for a given Monte Carlo simulation, the recovered parameters would have been very close to the input parameters. Thus, the procedure for fitting parameters to individual estimated spectra (which are all that are ever available) does not converge to the true parameters of the spectrum and does not recover these parameters. The error, of course, decreases as the number of degrees of freedom of the individual spectral estimates is increased.

10. Total Degrees of Freedom

A sample from a normal distribution with a zero mean of 16,384 (8192) values (16(8) $\times$ 1024) that were independent in the probability sense would yield a chi square distributed estimate of the variance with 16,384 (8192) degrees of freedom. The confidence interval on the estimate of the variance would be $\pm$1.8 (2.6)%.

The values used in the computation of the variance of an ocean wave record as in (6) are not independent. The areas under the individual sample spectra are random variables, and the area under the spectrum in Figure 5 is also a random variable. The distribution of these estimates of the variance

TABLE 3. Summary of Some of the Results of *Günther* [1981]

	Spectrum I			Spectrum II			Spectrum III		
		Output			Output			Output	
Parameter	Input	Theory‡	MC†	Input	Theory‡	MC†	Input	Theory‡	MC†
f^*_m	16.6	16.7	16.9	48.6	48.9	48.9	25.60	26.1	26.00
α	1.00	1.00	0.88	1.00	0.988	0.953	1.00	1.02	0.98
γ	3.30	3.60	4.02	3.30	4.21	4.61	1.00	1.46	1.50
σ_a	0.07	0.0706	0.0802	0.07	0.0551	0.0587	—	NOT FOUND	
σ_b	0.09	0.0793	0.0843	0.09	0.0666	0.0725	—	NOT FOUND	

* Theoretical results.
† Monte Carlo results.

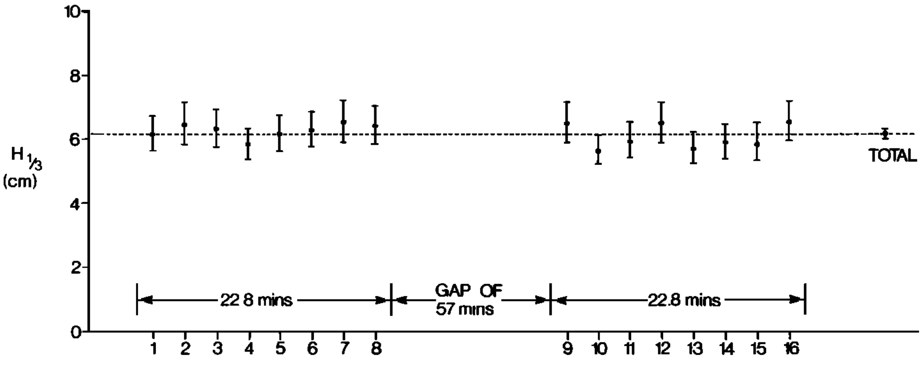

Fig. 8*a*. (Laboratory) Sampling variability of the significant wave height. The dashed line represents the estimate from the complete data set.

of a time history is not known. However, it can be approximated.

It must be assumed that the spectrum is a slowly varying function of frequency. This yields the various frequency smoothed spectra in Figure 4. Each independent estimate (every ninth value) then has a chi square distribution with the degrees of freedom given by twice the number of values of C_q^2 that are used (in the smoothing), say, D and an unknown parameter. If the unknown parameter does not change, as for the average over the 16 (8) sample spectra to get $\hat{S}_{ga}(q/N\Delta t)$, the chi square distributions compound and 18 degrees of freedom become 288 (144) degrees of freedom over a relatively narrow frequency band of nine elemental estimates.

Since the spectrum does vary from one nine element frequency band to another nine element band, the unknown parameters vary from part one of the spectrum to another, and the chi square estimates cannot be compounded. The moment generating functions (mgf's) for each independent band can be found. They will correspond to Chi Square mgf's, each with a different unknown parameter (the integral of the true spectrum over that band). The product of these different mgf's is then the mgf of the probability density function of the estimated variance. This product of moment generating functions cannot be inverted to obtain an analytical form for the desired probability density function.

However, this product of mgf's can be approximated by the mgf of a chi square distribution with a newly chosen unknown parameter and a different number for the total degrees of freedom. This approximation for the total degrees of freedom is given by (23)

$$\mathrm{TDF} \cong D \frac{(\Sigma S(f_r))^2}{\Sigma (S(f_r))^2} \tag{23}$$

For large values of the TDF, an additional fact makes the computation of the 90% confidence intervals quite simple. The confidence interval for the estimate of the variance is given by (24)

$$P(10^{-(\mathrm{TDF})^{-1/2}}\, \hat{\mathrm{var}} < \mathrm{var} < 10^{+(\mathrm{TDF})^{-1/2}}\, \hat{\mathrm{var}}) = 0.90 \tag{24}$$

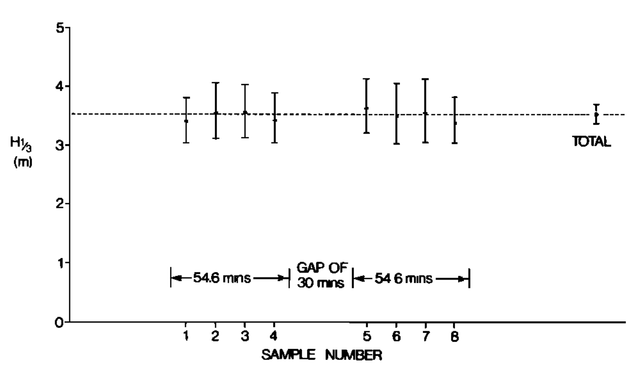

Fig. 8*b*. (Field) Sampling variability of the significant wave height. The dashed line represents the estimate from the complete data set.

TABLE 4. Estimates of Significant Height

	TDF	Lower (5% c.l.)	$\hat{H}_{1/3}$ (cm)	Upper (95% c.l.)	Within c.l.
			Laboratory		
Sample					
1	172	5.65	6.17	6.74	yes
2	128	5.83	6.46	7.15	yes
3	143	5.74	6.32	6.96	yes
4	197	5.38	5.84	6.34	yes
5	159	5.62	6.16	6.75	yes
6	181	5.78	6.30	6.86	yes
7	129	5.90	6.53	7.23	yes
8	166	5.87	6.42	7.02	yes
9	147	5.91	6.50	7.15	yes
10	195	5.22	5.67	6.16	low
11	162	5.46	5.98	6.55	yes
12	138	5.89	6.50	7.17	yes
13	172	5.25	5.73	6.26	yes
14	157	5.40	5.92	6.49	yes
15	131	5.33	5.89	6.51	yes
16	153	5.98	6.56	7.20	yes
Sum	2530				
Total	2840	6.06	6.19	6.33	
			Field		
Sample					
1	101	3.04	3.41	3.82	yes
2	72	3.10	3.55	4.07	yes
3	84	3.12	3.54	4.01	yes
4	78	3.01	3.43	3.91	yes
5	80	3.20	3.64	4.14	yes
6	60	3.02	3.50	4.06	yes
7	59	3.06	3.56	4.14	yes
8	93	3.02	3.40	3.83	yes
Sum	627				
Total	649	3.37	3.53	3.69	

The significant wave height can be computed from (25)

$$\hat{H}_{1/3} = 4(\hat{\text{var}})^{1/2} \tag{25}$$

The confidence interval on the significant wave height is given by (26)

$$P((10^{-(\text{TDF})^{-1/2}})^{1/2}\hat{H}_{1/3} < H_{1/3} < (10^{+(\text{TDF})^{-1/2}})^{1/2}\hat{H}_{1/3}) = 0.90 \tag{26}$$

The significant wave heights for each of the 16 (8) samples and for the total sample are given in Table 4 and graphed versus sample number in Figure 8. The values for the total degrees of freedom for each sample were computed by means of (23) by starting with the estimate at the spectral peak and by using every ninth value toward both lower and higher frequencies in the range $0.76\ f_m < f < 1.4\ f_m$. Spectral values outside of this range had a negligible effect on (23). From these estimates of the total degrees of freedom, the confidence intervals on the estimated significant wave heights were found for each sample and for the total sample.

The sum of the TDF's for the 16 (8) samples does not equal the TDF for the total sample. It is 89 (97)% of that value. This discrepancy is not too serious. Large changes in the total degrees of freedom are needed to obtain appreciably different ranges for the confidence intervals.

For the 16 (8) samples, the significant wave height is essentially unknown to within ±0.6 cm (0.5 m) out of about 6.2 cm (3.5 m) for an uncertainty of ±10 (14)%. The largest value for the upper confidence limit is 7.23 cm (4.14 m), and the smallest value for the lower confidence limit is 5.22 cm (3.01 m) for a range of 2.01 cm (1.13 m), or 32 (32)% of the significant height of 6.19 cm (3.53 m) from the total sample.

The last column in Table 4 shows whether or not the confidence interval on the significant height for each sample encloses the significant height for the total sample.

If 6.19 cm (3.53 m) were the 'true' value of the significant wave height, then each of the 16 (8) intervals has an a priori probability of 0.90 of enclosing this 'true' value. Fifteen (eight) of the 16 (8) do enclose the assumed 'true' value. The probability of this happening is 0.51 (0.43) for 15 or more (and for all 8).

Figure 8 illustrates these features in another way. The confidence intervals for all but 1 (0) of the 16 (8) estimates enclose the overall average value represented by a dashed line.

The main conclusions are, however, quite simple. The 1024 values for each sample are worth only about 160 (78) independent values for the estimation of the variance. The 16,384 (8192) values for the total sample are worth only 2840 (649) independent observations for the estimation of the variance.

11. EFFECTS OF DECREASED RESOLUTION

Smoothing an FFT by a running average serves to emphasize the effects of sampling variability because of the irregu-

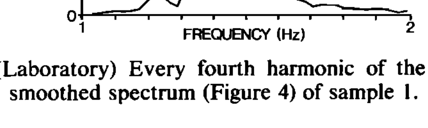

Fig. 9*a*. (Laboratory) Every fourth harmonic of the nine-point smoothed spectrum (Figure 4) of sample 1.

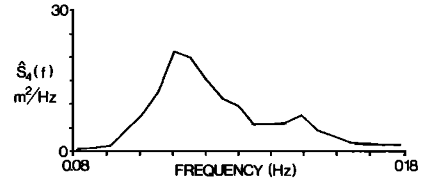

Fig. 9*b*. (Field) Every fourth harmonic of the nine-point smoothed spectrum (Figure 4) of sample 5.

larities that result in graphs such as those in Figure 4. Many wave records have been analyzed by means of the methods described in *Tukey* [1949] and *Blackman and Tukey* [1958].

These analysis procedures yielded far fewer values along the frequency axis, and therefore gave the impression that the spectra were much smoother.

As an example, the values of $\hat{S}_a(f)$ for sample 1 (5) have been plotted for every fourth harmonic between 171 (66) and 339 (146) in Figure 9 to be compared with the corresponding complete plot in Figure 4.

Every other point in this figure is nearly independent as they would be in a Tukey-type analysis. Spectra in this form may compound the problem of the effects of sampling variability by masking it.

12. CONCLUSIONS

The effects of sampling variability in the estimation of spectra of wind-generated waves have been studied by means of 16 samples obtained in a wind-water tunnel at a constant wind and fetch and eight samples from Lake Ontario at virtually constant wind and fetch. The effects of sampling variability are as predicted by the theory of stationary Gaussian processes. They are appreciable for record lengths comparable to a 17-min record obtained at sea.

In particular, the significant wave height is not known to within ±10–15% of an estimated value, and the spectral peak is typically an overestimate of a value that would be obtained from a larger sample. Also, the frequency of the peak is not known to within a range of ±5%, or so, of its true value.

Acknowledgments. The authors acknowledge the assistance of D. Beesley, J. Carew, and T. Nudds in the collection of field and laboratory data. The contribution of W. J. Pierson was supported in part by the Coastal Waves Program of the National Ocean Survey, NOAA, under contract NA 81AA-D-00060.

REFERENCES

Blackman, R. B., and J. W. Tukey, The measurement of power spectra from the point of view of communications engineering. *Bell System Tech. J.*, *37*, 1958.

Cooley, J. W., and J. W. Tukey, An algorithm for the machine calculation of complex Fourier series, *Math. Comput.*, *19*, 297–307, 1965.

Cooley, J. W., P. A. W. Lewis, and P. D. Welch, Historical notes on the fast Fourier transform, *IEEE Transl. Audio Electroacoust.*, *Au-15*, 76–77, 1967.

Donelan, M. A., K. N. Birch, and D. C. Beesley, Generalized profiles of wind speed, temperature and humidity, paper presented at Proceedings 17th Conference Great Lakes Research, Internat. Assoc. Great Lakes Res., Hamilton, Ont., 1974.

Günther, H., A parametric surface wave model and the statistics of the prediction parameters, *Hamburger Geophys. Einzelschr.*, *55*, 1–90, 1981.

Hasselmann, K., D. B. Ross, P. Muller, and W. Sell, A parametric wave prediction Model, *J. Phys. Oceanogr.*, *6*, 200–228, 1976.

Hasselmann, K., T. P. Barnett, E. Bouws, H. Carlson, D. E.

Cartwright, K. Enke, J. A. Ewing, H. Gienapp, D. E. Hasselmann, P. Kruseman, A. Meerburg, P. Müller, D. J. Olbers, K. Richter, W. Sell, and H. Walden, Measurements of wind-wave growth and swell decay during the Joint North Sea Wave Project (JONSWAP), *Deutsch Hydrogr. Z., A8* (suppl.), 1–95, 1973.

Mitsuyasu, H., Y. Y. Kuo, and A. Masuda, The dispersion relation for wind waves in decay area, in *Turbulent Fluxes Through the Sea Surface, Wave Dynamics and Prediction, NATO Conf. Ser.*, edited by A. Favre, and K. Hasselmann, pp. 221–234, Plenum, New York, 1978.

Neumann, G., and W. J. Pierson, Jr., *Principles of Physical Oceanography*, Prentice-Hall, Englewood Cliffs, N.J., 1966.

Pierson, W. J., Comments on 'A parametric wave prediction model,' *J. Phys. Oceanogr., 7,* 127–134, 1977.

Pierson, W. J., Comments on 'Distribution and steepness of ripples on carrier waves,' *J. Phys. Oceanogr., 10,* 1882–1883, 1980.

Pierson, W. J., and W. Marks, The power spectrum analysis of ocean-wave records, *Eos Trans. AGU, 33,* 834–844, 1952.

Pierson, W. J., Jr., and L. Moskowitz, A proposed spectral form for fully developed wind seas based on the similarity theory of S. A. Kitaigorodskii, *J. Geophys. Res., 69,* 5181–5190, 1964.

Resch, F., and J. P. Selva, Experimental study of momentum transfer, heat and water vapor fluxes under different stability conditions, in *Turbulent Fluxes Through the Sea Surface, Wave Dynamics and Prediction, NATO Conf. Ser.*, edited by A. Favre, and K. Hasselmann, pp. 81–98, Plenum, New York, 1978.

Tukey, J. W., The sampling theory of power spectrum estimates. Symposium on applications of autocorrelation analysis to physical problems, *NAV EXOS-P-735,* Off. of Nav. Res., Woods Hole, Mass., 1949.

Wu, J., Distribution and steepness of ripples on carrier waves, *J. Phys. Oceanogr., 9,* 1014–1021, 1979.

Wu, J., Reply to Pierson, 1980, *J. Phys. Oceanogr., 10,* 1883–1884, 1980.

(Received May 12, 1982;
revised January 24, 1983;
accepted January 25, 1983.)